

Correlation between saturation magnetization, bandgap, and lattice volume of transition metal (M=Cr, Mn, Fe, Co, or Ni) doped Zn_{1-x}M_xO nanoparticles

J. Anghel, A. Thurber, D. A. Tenne, C. B. Hanna, and A. Punnoose^{a)}

Department of Physics, Boise State University, Boise, Idaho 83725-1570, USA

(Presented 19 January 2010; received 30 October 2009; accepted 8 February 2010; published online 7 May 2010)

This work reports on transition metal doped ZnO nanoparticles and compares the effects doping with different transition metal ions has on the structural, optical, and magnetic properties. Zn_{1-x}M_xO (M=Cr, Mn, Fe, Co, or Ni) nanoparticles were prepared by a chemical process for $x=0.02$ and 0.05 in powder form. The powders were characterized by x-ray diffraction (XRD), spectrophotometry, and magnetometry. The Zn_{1-x}M_xO samples showed a strong correlation between changes in the lattice parameters, bandgap energy, and the ferromagnetic saturation magnetization. Unit cell volume and bandgap, determined from XRD and spectrophotometry respectively, were maximized with Fe doping and decreased as the atomic number of the dopant moved away from Fe. Bandgap was generally lower at $x=0.05$ than $x=0.02$ for all dopants. The saturation magnetization reached a maximum of 6.38 memu/g for Zn_{0.95}Fe_{0.05}O. © 2010 American Institute of Physics. [doi:10.1063/1.3360189]

Ferromagnetism above room temperature has already been predicted theoretically¹⁻³ and reported experimentally⁴⁻⁶ for transition metal dopants in ZnO in both powders and thin films. Various reports have argued that the ferromagnetic properties of transition metal doped metal oxides strongly depend on the metal oxide host system, surface defects, particle size, transition metal dopant type, and concentration.⁷⁻⁹ Interestingly, Venkatesan *et al.*⁹ have shown that in transition metal doped zinc oxide thin films, the highest magnetic moment is observed for Co doping; however, these reports focus only on thin films and not nanoparticle powders as in this work. Recently, others have claimed that ferromagnetism can be obtained at room temperature in thin films or nanoparticles of pure nonmagnetic metal oxides, and that the ferromagnetic properties do not depend on the transition metal dopant.¹⁰⁻¹³ Because of these conflicting reports, we have prepared a series of doped ZnO nanoparticles using a chemical route and compared the ferromagnetism of Zn_{1-x}M_xO nanoparticles as a function of the transition metal dopant type (M=Cr, Mn, Fe, Co or Ni) while leaving the preparation method, surface structure, particle size, dopant concentration (2% and 5%), and host system unchanged. Our studies clearly suggest that the ferromagnetic properties of Zn_{1-x}M_xO nanoparticles strongly depend on the transition metal dopant and that the ferromagnetic moment is strongest for Fe doping, details of which are presented below.

The synthesis method has been reported elsewhere but was extended and modified in some parts.¹⁴ Zn(OOCCH₃)₂·2H₂O, LiOH, and transition metal nitrates were dissolved in 100 ml of ethanol, heated, and then maintained at 70 °C for 90 min. The solution was then allowed to

cool for 120 min before adding 100 ml of N-Heptane. The mixture was then aged for 24 h, after which the particles were removed by centrifugation and washed in a water-ethanol-water cycle to remove any unwanted reaction byproducts.¹⁵ After washing, the samples were dried in an oven for 12 h at 50 °C. The amount of Zn(OOCCH₃)₂·2H₂O and transition metal nitrates used were regulated to maintain the total ion concentration in solution.

X-ray diffraction (XRD) was performed using a Philips X'Pert MPD diffractometer in Bragg-Brentano geometry. The system uses a Cu K_α x-ray source ($\lambda=1.5418$ Å). Diffuse reflectance was measured on a Varian Cary 5000 UV-Vis-NIR spectrophotometer from 200–800 nm. Magnetometry was performed at room temperature using a Lakeshore 7404 vibrating sample magnetometer (VSM). Powder samples were tightly packed into a clear straw and mounted to the VSM.

Samples were prepared for $x=0.02$ and 0.05 , three times for each dopant, in order to obtain a statistical average and to demonstrate repeatability. The resulting powders were studied by XRD, spectrophotometry, and magnetometry to rule out the presence of any impurity phases and to characterize their structure, morphology, electronic, and magnetic properties.

XRD patterns, shown in Fig. 1(a), demonstrate the structure to be single-phase wurzite ZnO with no evidence of any secondary phases. Crystallite sizes for all samples were estimated to be about 6.9 ± 1.4 nm, as determined by the Scherrer relation using the (102) peak of ZnO. This confirms that any variation in the properties of the Zn_{1-x}M_xO samples with different transition metal ions is not due to any differences in the crystallite sizes. Unit cell volume gave a maximum for Fe, as seen in Fig. 1(b), dropping down as the atomic number of the dopant moved away from that of Fe. The observed changes were dominated by changes in lattice parameter a .

^{a)}Electronic mail: apunnoos@biosestate.edu.

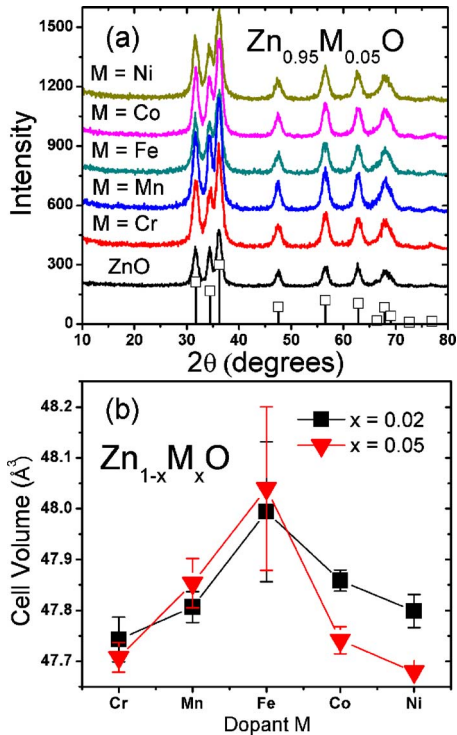


FIG. 1. (Color online) (a) Representative XRD patterns for Zn_{0.95}M_{0.05}O (M=Ni, Co, Fe, Mn, and Cr), along with pure ZnO nanoparticles made by the same method. Drop lines show reference peak positions and relative intensities for ZnO. (b) Unit cell volume for Zn_{0.95}M_{0.05}O and Zn_{0.98}M_{0.02}O (M=Ni, Co, Fe, Mn, and Cr). Error bars shown are standard deviations, after taking average of three independently prepared samples. Connecting lines shown for visual aid.

The unit cell volume of pure ZnO nanoparticles of similar size made by the same chemical method was measured at $47.83 \pm 0.04 \text{ \AA}^3$, while bulk ZnO has a unit cell volume of 47.58 \AA^3 .¹⁶ All of the nanoparticle samples show an expansion of the crystal lattice relative to the bulk sample, while Fe causes the most additional expansion. As the percentage of dopant increases the unit cell volume shift more proportional to the ionic radii [see Fig. 1(b)]; Mn (0.8 Å) and Fe (0.77 Å) having larger ionic radii than Zn (0.74 Å), and Cr (0.73 Å), Co (0.72 Å), and Ni (0.69 Å) have smaller radii than Zn.^{17,18} Others have also reported seeing similar deformation of lattice structure as a result of doping ZnO nanoparticles with transition metals.^{19–21}

Bandgap was measured using diffuse reflectance spectroscopy [see Fig. 2(a)] following the Kubelka–Munk method.^{22,23} For both 2% and 5% M doping concentrations, there is a peak in bandgap energy observed for Fe doped samples. The 5% M doped samples all demonstrated lower bandgaps than their 2% M counterparts [see Fig. 2(b)], while maintaining a maximum for Fe. The peak at Fe in bandgap is very similar to the observed changes in the unit cell volume. The trend observed here between unit cell volume and bandgap may be explained by the bandgap being directly proportional to interatomic separation, although it is also possible that new states are being introduced by the dopant presence. However, without knowing the oxidation state, coordination numbers, or if the dopant is interstitial or substitutional it is difficult to explicitly determine the effect on structure.

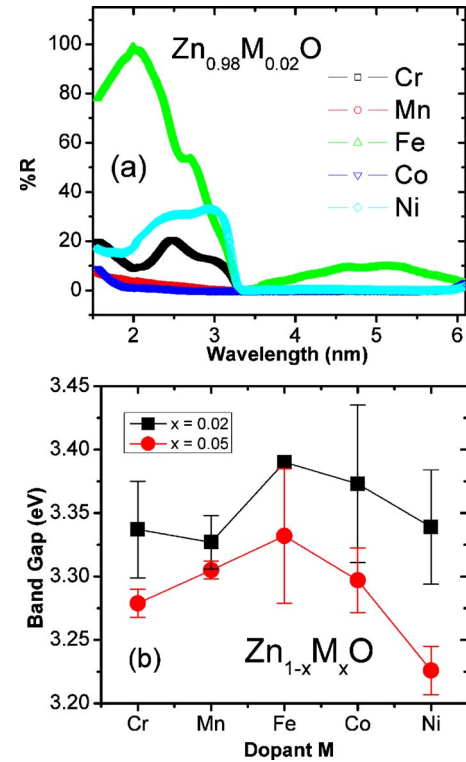


FIG. 2. (Color online) Optical data collected on transition-metal-doped ZnO. (a) Representative Kubelka–Munk transformed diffuse reflectance data collected in air at room temperature on powders of Zn_{0.98}M_{0.02}O (M=Ni, Co, Fe, Mn, and Cr). (b) Bandgap as determined from diffuse reflectance data for 2 and 5 at. % transition-metal-doped ZnO. Error bars shown are standard deviation after taking average of three independently prepared samples. Connecting lines shown for visual aid.

Magnetization M versus magnetic field H , measured at room temperature for $x=0.02$, revealed that weak ferromagnetic behavior is evident in all the transition metal doped ZnO particles. All the doped samples show open hysteresis loops, with Fe-doped ZnO showing the most prominent loop, and Ni and Cr showing the weakest, as seen in Fig. 3(a). The ferromagnetic properties are stronger for 5% doping and the relative strength with respect to each dopant mirrors the behavior observed for the 2% doping. This data shows that Fe is the most effective dopant for producing ferromagnetism in nanoparticles of ZnO at 2 and 5 at. % as seen in Figs. 3(b) and 3(c). This is a clearly visible trend, showing that the closer the atomic number of the transition metal acting as the dopant is to that of Fe, the larger the magnetization. Previous studies on Fe doped SnO₂ (Ref. 24) and Ni doped CeO₂ (Ref. 25) have shown evidence of interstitial dopant ions. Depending on the extent of interstitial doping and the oxidation state of the doped transition metal, free electron capture and hole doping might play a major role in varying the free electron concentration in the host system.²⁶ Since the observed magnetism is generally believed to be carrier (electron) mediated, the extent of magnetic coupling between the doped ions (and, therefore, the net magnetization) will depend on the availability of the free electrons and not just the magnetic moment of the dopant alone.

This peak at M=Fe corresponds to the similar peaks observed for unit cell volume and bandgap energy discussed above, suggesting that the observed changes in structure,

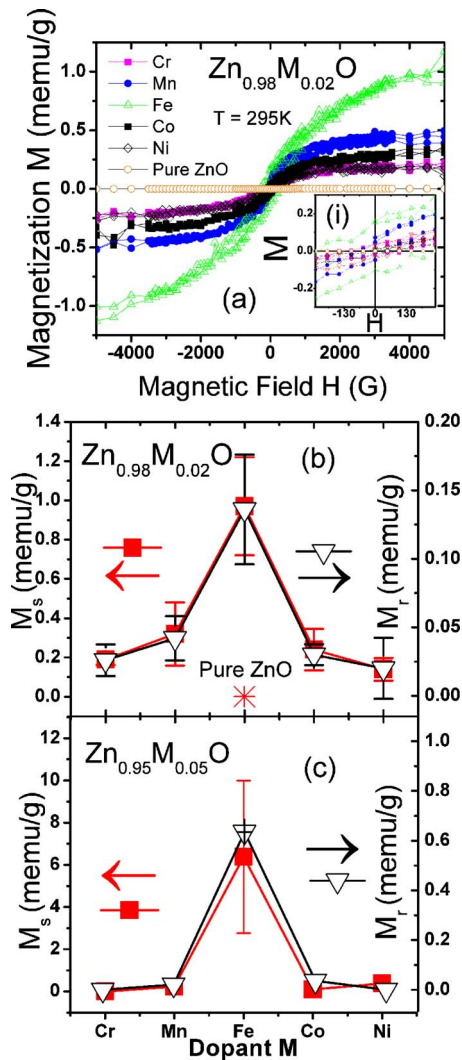


FIG. 3. (Color online) (a) Representative room temperature M vs H data on $\text{Zn}_{0.98}\text{M}_{0.02}\text{O}$ ($M = \text{Ni, Co, Fe, Mn, and Cr}$). Saturation magnetization M_s and magnetic remanence M_r for (b) $\text{Zn}_{0.98}\text{M}_{0.02}\text{O}$ and (c) $\text{Zn}_{0.95}\text{M}_{0.05}\text{O}$. Also shown in (b) is the value of the saturation magnetization measured for pure ZnO synthesized by the same method. Inset (i) shows the M vs H data near the origin to demonstrate the loops are open. Error bars shown are standard deviation after taking average of three independently prepared samples. Connecting lines shown for visual aid.

bandgap and magnetism are related and dependent on the transition-metal dopant. Similar correlations between magnetism, microstructure, and/or optically determined bandgap have been reported on other transition-metal doped metal-oxide systems.^{24–27} Such strong correlation of the ferromagnetic properties and the systematic changes in the structural and optical parameters of the host semiconductor confirms that, whether the change in magnetism is an indirect result of the dopant affecting the bandgap or structural properties or directly related only to dopant type, the observed ferromagnetism is ultimately transition metal dopant driven.

The above results suggest that the dopant type plays a crucial role in the physical properties of the $\text{Zn}_{1-x}\text{M}_x\text{O}$ nanoparticles investigated here. The systematic variation in dopant type (while maintaining size, synthesis method, surface structure, and dopant percentage) and the repeatability of

these experiments demonstrates that the effect is related to the intended transition-metal dopant, and cannot be attributed to any unaccounted impurity. The maximum magnetization corresponds to a similar maximum in unit cell volume determined by XRD and bandgap energy determined by diffuse reflectance; suggesting a strong correlation between the structural, optical, and magnetic properties as a function of transition-metal-dopant in ZnO nanoparticles.

This work was supported in part by the NSF-CAREER program (Grant No. DMR-0449639), DoE-EPSCoR program (Grant No. DE-FG02-04ER46142), ARO under Grant No. W911NF-09-1-0051, NSF-RUI (Grant No. DMR-0840227), and NSF-RUI (Grant No. DMR-0605652).

- ¹T. Dietl, H. Ohno, F. Matsukura, J. Cibert, and D. Ferrand, *Science* **287**, 1019 (2000).
- ²K. Sato and H. Katayama-Yoshida, *Physica B* **308–310**, 904 (2001).
- ³J. M. D. Coey, M. Venkatesan, and C. B. Fitzgerald, *Nature Mater.* **4**, 173 (2005).
- ⁴T. Fukumura, Z. Jin, M. Kawasaki, T. Shono, T. Hasegawa, S. Koshihara, and H. Koinuma, *Appl. Phys. Lett.* **78**, 958 (2001).
- ⁵N. S. Norberg, K. R. Kittilstved, J. E. Amonette, R. K. Kukkadapu, D. A. Schwartz, and D. R. Gamelin, *J. Am. Chem. Soc.* **126**, 9387 (2004).
- ⁶D. Norton, M. Overberg, S. Pearton, K. Pruessner, J. Budai, L. Boatner, M. Chisholm, J. Lee, Z. Khim, Y. Park, and R. Wilson, *Appl. Phys. Lett.* **83**, 5488 (2003).
- ⁷N. Theodoropoulou, A. Hebard, D. Norton, J. Budai, L. Boatner, J. Lee, Z. Khim, Y. Park, M. Overberg, S. Pearton, and R. Wilson, *Solid-State Electron.* **47**, 2231 (2003).
- ⁸A. Gupta, H. Cao, K. Parekh, K. Rao, A. Raju, and U. Waghmare, *J. Appl. Phys.* **101**, 09N513 (2007).
- ⁹M. Venkatesan, C. B. Fitzgerald, J. G. Lunney, and J. M. D. Coey, *Phys. Rev. Lett.* **93**, 177206 (2004).
- ¹⁰A. Sundaresan, R. Bhargavi, N. Rangrajan, U. Siddesh, and C. N. R. Rao, *Phys. Rev. B* **74**, 161306 (2006).
- ¹¹D. Gao, Z. Zhang, J. Fu, Y. Xu, J. Qi, and D. Xue, *J. Appl. Phys.* **105**, 113928 (2009).
- ¹²M. A. Garcia, J. M. Merino, E. Fernandez Pinel, A. Quesada, J. de la Venta, M. L. Ruiz Gonzalez, G. R. Castro, P. Crespo, J. Llopis, J. M. Gonzalez-Calbet, and A. Hernando, *Nano Lett.* **7**, 1489 (2007).
- ¹³S. Kumar, Y. J. Kim, B. H. Koo, S. Gautam, K. H. Chae, R. Kumar, and C. G. Lee, *Mater. Lett.* **63**, 194 (2009).
- ¹⁴L. Spanhel and M. Anderson, *J. Am. Chem. Soc.* **113**, 2826 (1991).
- ¹⁵E. Meulenkamp, *J. Phys. Chem. B* **102**, 5566 (1998).
- ¹⁶H. E. Swanson and R. K. Fuyat, *Natl. Bur. Stand. Circ. (U. S.)* **2**, 25 (1953).
- ¹⁷S. T. Breviglieri, E. T. G. Cavalherio, and G. O. Chierice, *Thermochim. Acta* **356**, 79 (2000).
- ¹⁸B. K. Roberts, A. B. Pakhomov, V. S. Shutthanandan, and K. M. Krishnan, *J. Appl. Phys.* **97**, 10D310 (2005).
- ¹⁹S. Senthilkumar, K. Rajendran, S. Banerjee, T. K. Chini, and V. Sengodan, *Mater. Sci. Semicond. Process.* **11**, 6 (2008).
- ²⁰M. L. Dinesha, H. S. Jayanna, S. Mohanty, and S. Ravi, *J. Alloys Compd.* **480**, 618 (2008).
- ²¹B. Wang, J. Iqbal, X. Shan, G. Huang, H. Fu, R. Yu, and D. Yu, *Mater. Chem. Phys.* **113**, 103 (2009).
- ²²P. Kubelka and F. Munk, *Tech. Phys.* **12**, 593 (1931).
- ²³P. Kubelka, *J. Opt. Soc. Am.* **38**, 448 (1948).
- ²⁴A. Punnoose, J. Hays, A. Thurber, M. H. Engelhard, R. K. Kukkadapu, C. Wang, V. Shutthanandan, and S. Thenvuthasan, *Phys. Rev. B* **72**, 054402 (2005).
- ²⁵A. Thurber, K. M. Reddy, V. Shutthanandan, M. H. Engelhard, C. Wang, J. Hays, and A. Punnoose, *Phys. Rev. B* **76**, 165206 (2007).
- ²⁶C. Van Komen, A. Punnoose, and M. S. Seehra, *Solid State Commun.* **149**, 2257 (2009).
- ²⁷J. Hays, A. Punnoose, R. Baldner, M. H. Engelhard, J. Peloquin, and K. M. Reddy, *Phys. Rev. B* **72**, 075203 (2005).